

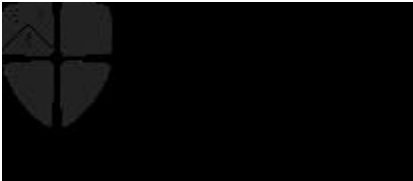
X-ray Probes of the Layer and Interface Structure of Nanoscale Films for Electronics and Spintronics

Brian K Tanner (and others)

Bede plc, Belmont Business Park, Durham

and

Department of Physics, Durham University





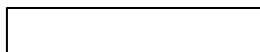
Opto-electronic Materials

Driver for High Resolution X-ray Diffraction

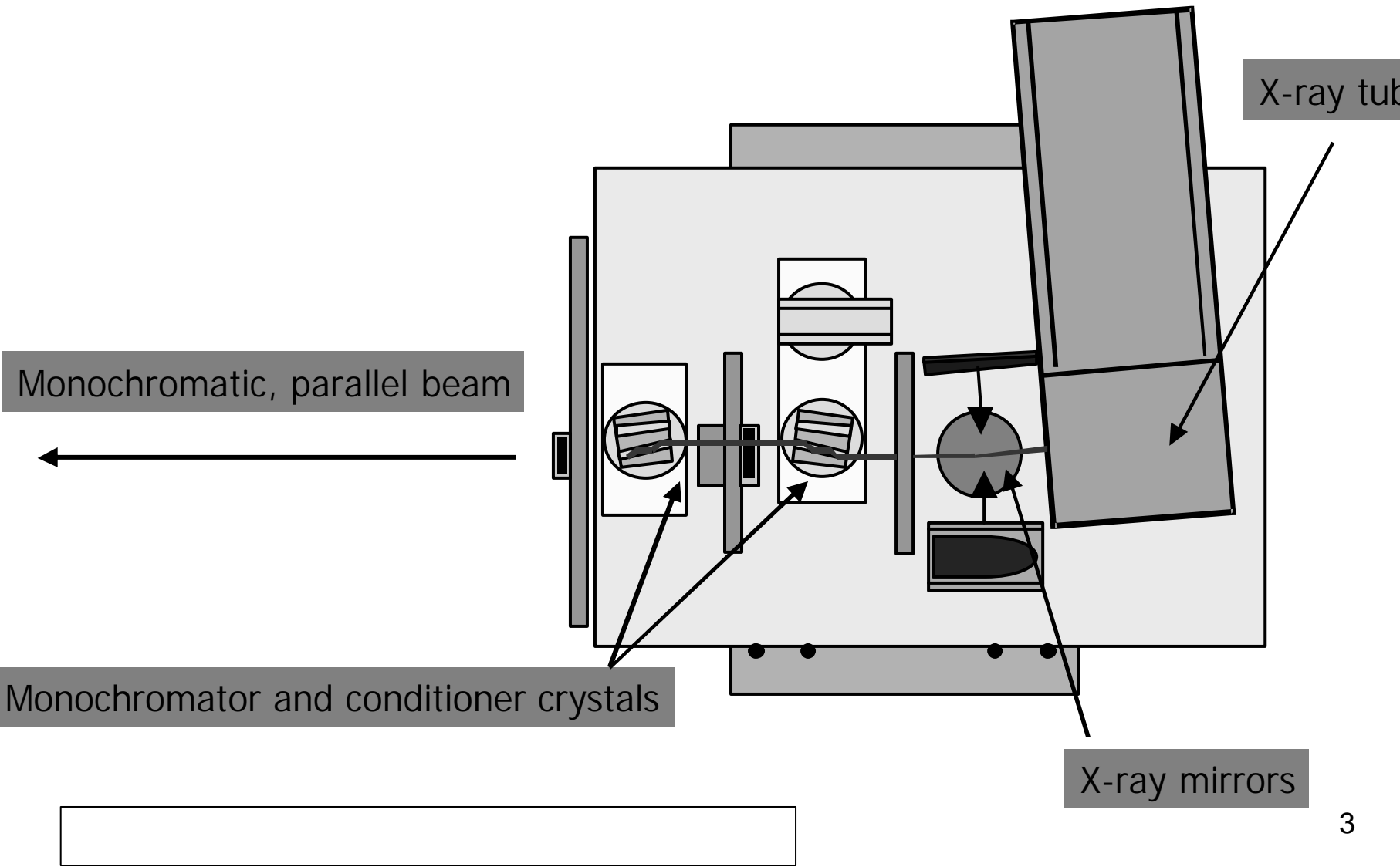
Development in 1980s

- $\text{In}_x\text{Ga}_{1-x}\text{As}_y\text{P}_{1-y}$ for PIN diodes for long-haul telecoms
- $\text{Al}_x\text{Ga}_{1-x}\text{As}$ for laser diodes

Measurement of composition

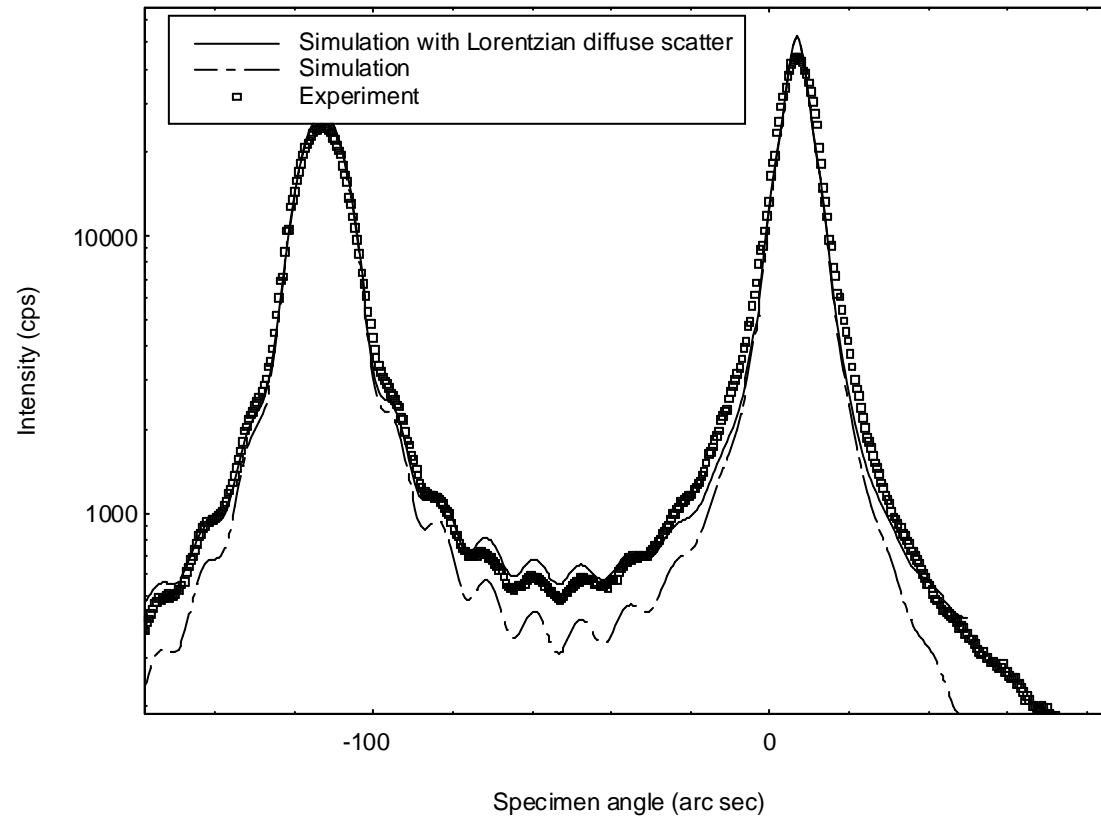


High Resolution X-ray Diffraction





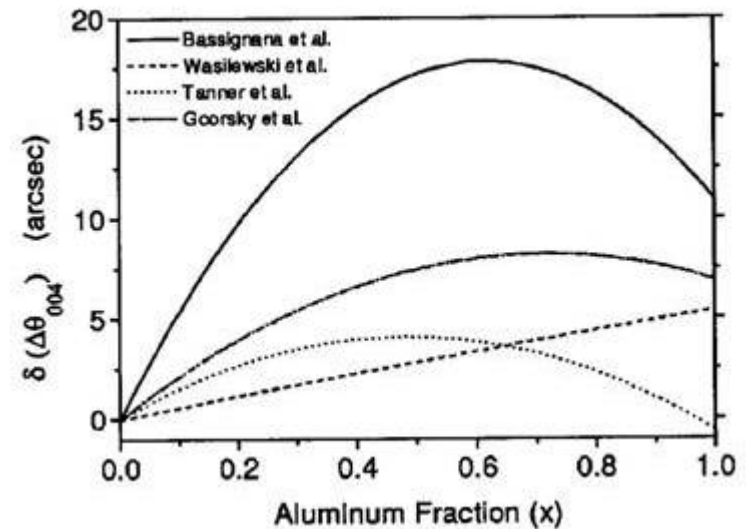
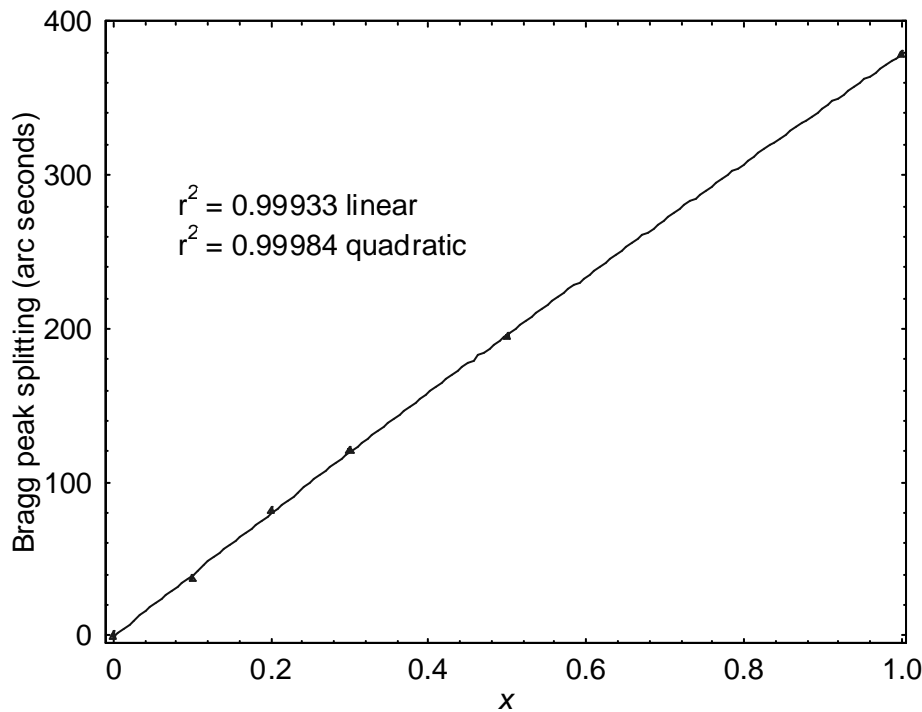
Composition of $\text{Al}_x\text{Ga}_{1-x}\text{As}$ on GaAs



Measure splitting between substrate and layer
Assume Vegard's Law (linear interpolation) to get x

Composition of $\text{Al}_x\text{Ga}_{1-x}\text{As}$ on GaAs

B K Tanner *et al* Appl Phys Lett **59** (1981) 2272



Quadratic dependence
4 arc seconds \cong 1% Al

S Gehrsitz *et al* Phys Rev B **60** (1999) 11601

Takagi-Taupin formulation of X-ray Dynamical Diffraction Theory

$$\frac{I}{i p} \frac{\mathcal{I} D_0}{\mathcal{I} s_0} = c_0 D_0 + C c_{-h} D_h$$

$$\frac{I}{i p} \frac{\mathcal{I} D_h}{\mathcal{I} s_h} = (c_0 - a_h) D_h + C c_h D_0$$

a_h is the deviation of the incident wave from the exact Bragg condition

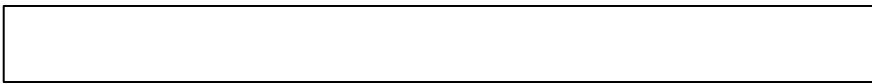
s_0 and s_h are **unit** vectors in the directions of \mathbf{K}_0 and \mathbf{K}_h

C is the polarisation factor

χ_0 and χ_h are the electric susceptibilities

(these describe the crystal)

$$c_h = -\frac{r_e I^2}{p V} F_h$$



Recursion relation format

M A G Halliwell, J Juler and A G Norman, Inst Phys Conf Ser 67 (1983) 365
 M G A Halliwell, M A G Lyons and M J Hill, J Crystal Growth 68 (1984) 523

$$A = Cc_{-h} \quad B = \frac{(1-b)c_0}{2} + \frac{a_h p}{2} \quad D = \frac{p}{lg_0} \quad E = -Cb g_h \quad F = \sqrt{BB - EA}$$

where $b = \gamma_o / \gamma_h$.

Amplitude ratio $X = D_h / D_o$,

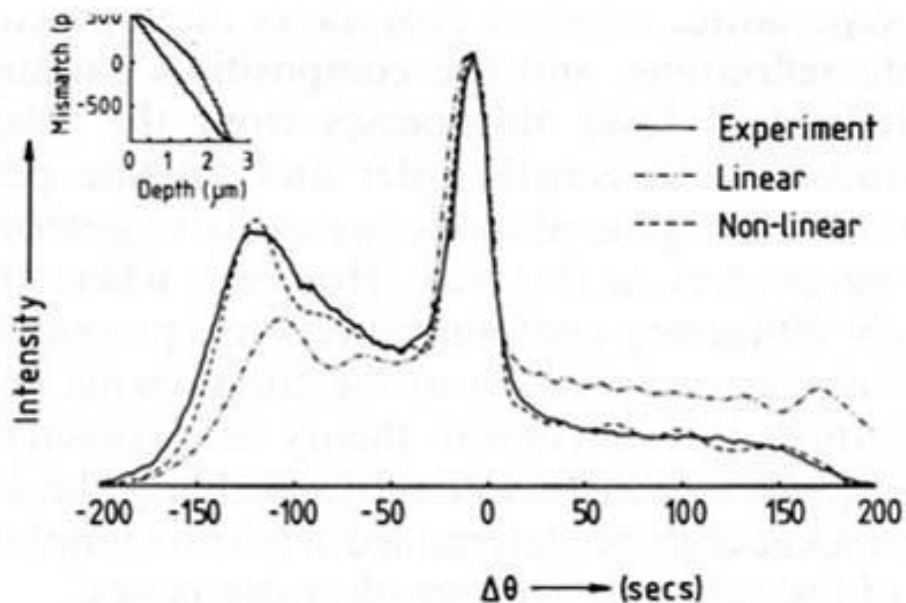
$$X = \frac{X' F + i(BX' + E) \tan(DF(z - w))}{F - i(AX' + B) \tan(DF(z - w))}$$

z is depth above the depth w at which the amplitude ratio is the known value X'



Recursion relation format

M J Hill, B K Tanner, M A G Halliwell and M H Lyons *J Appl Cryst* **18** (1985) 446



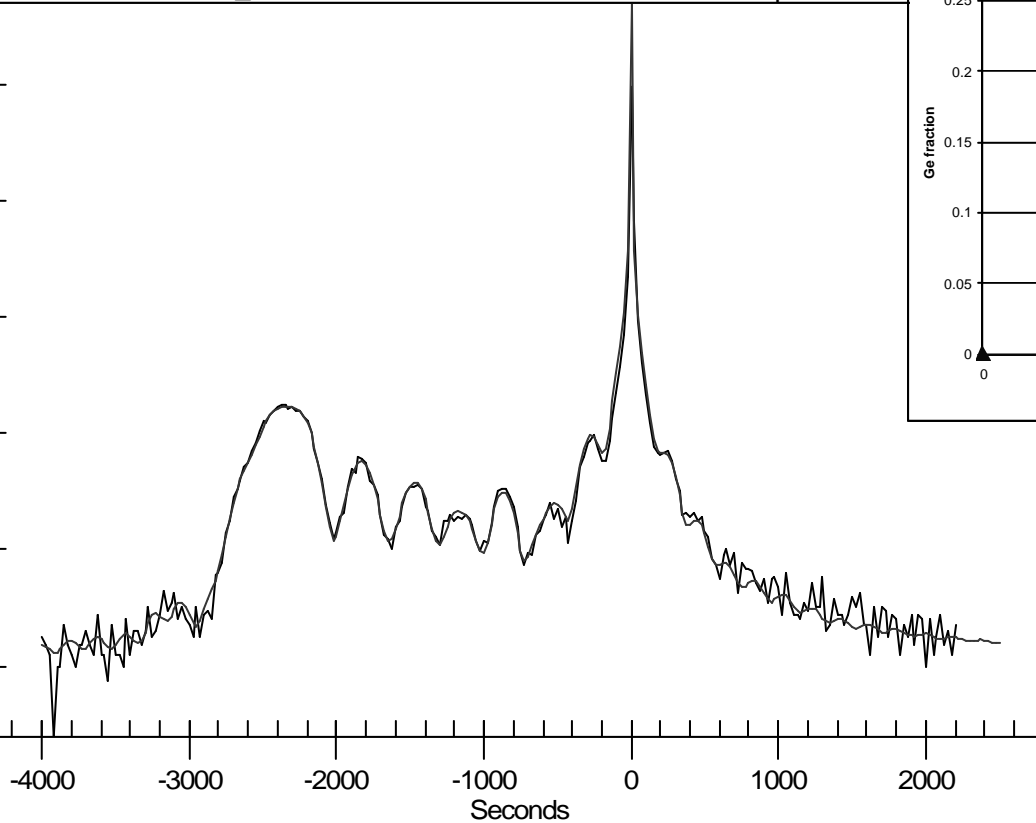
Fit to a graded 2.3 μm GaInAs layer, nominally lattice matched to InP
Note mismatch of only several hundred ppm

Graded SiGe structure (blanket)

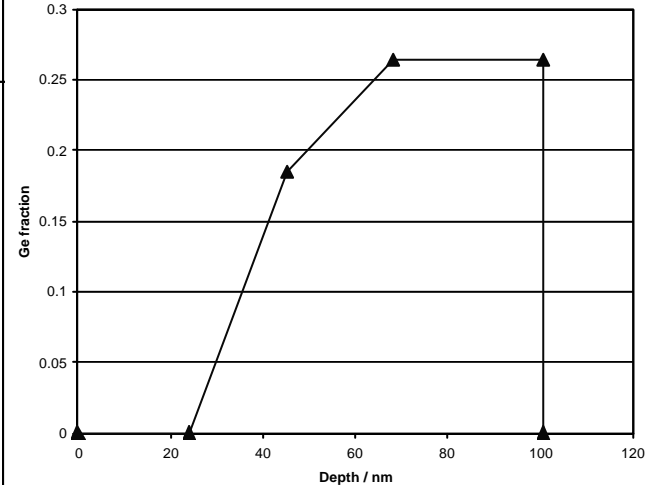
slot-23_0aa1.x01

temp.sim

Intensity (log scale)



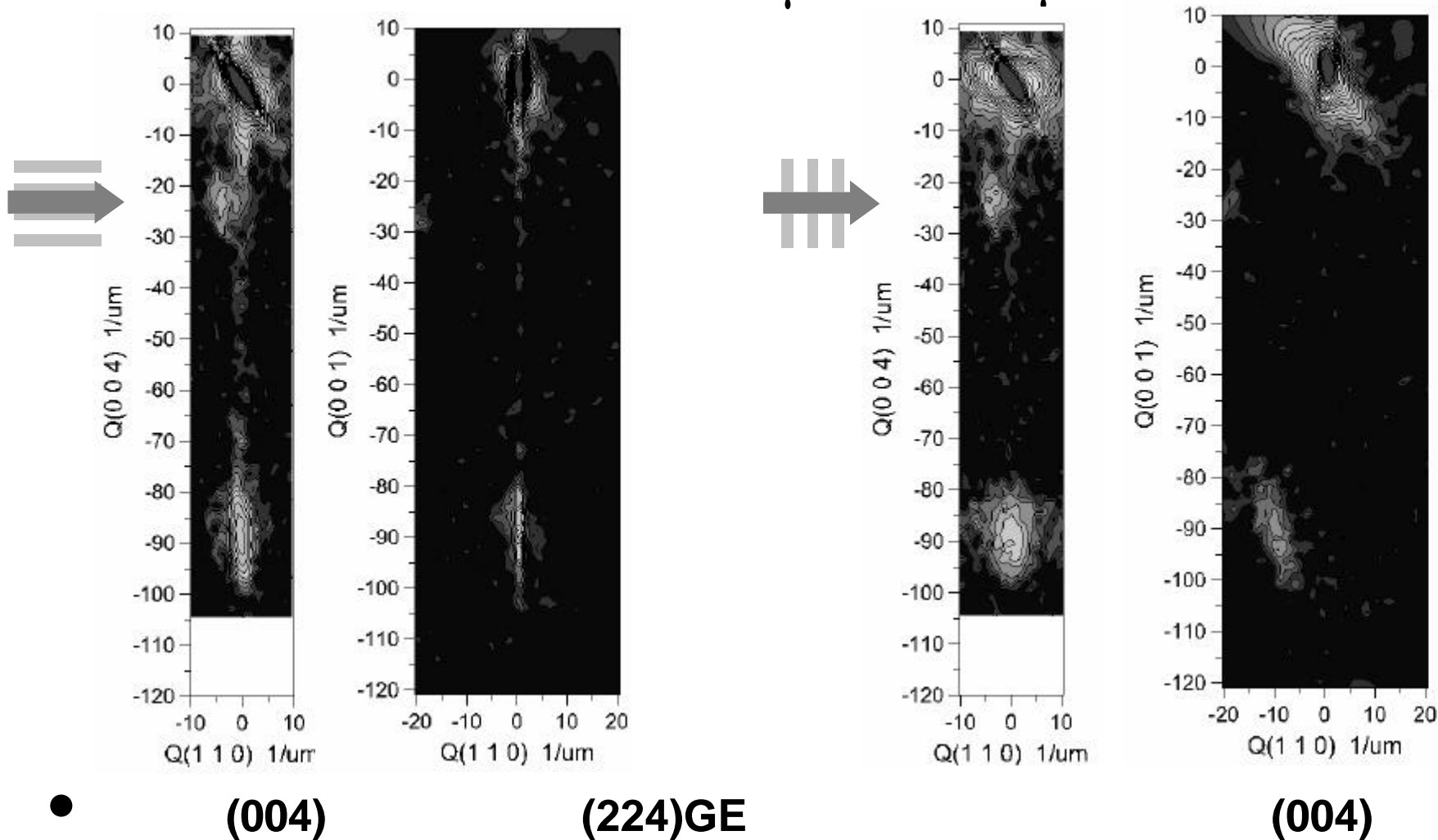
Ge profile for Slot 23



**QC200
diffractometer +
bede RADS
Mercury auto-
fitting software**

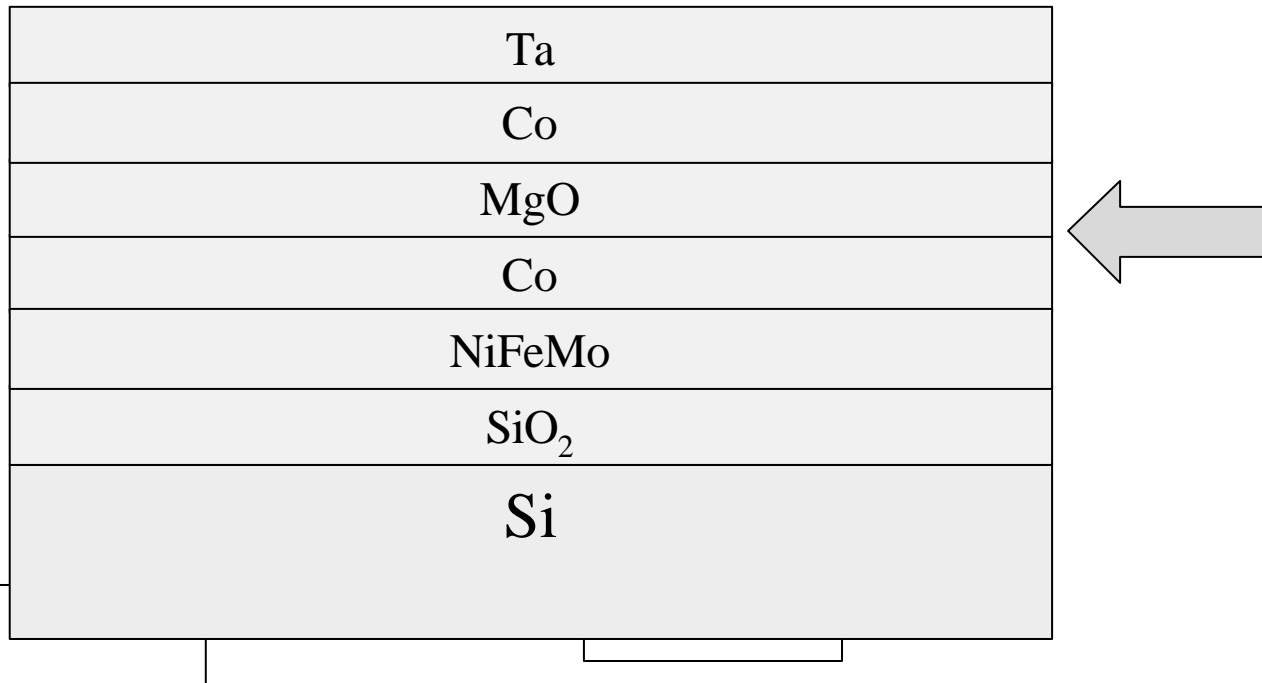
sample courtesy Hitachi-Kokusai Electric

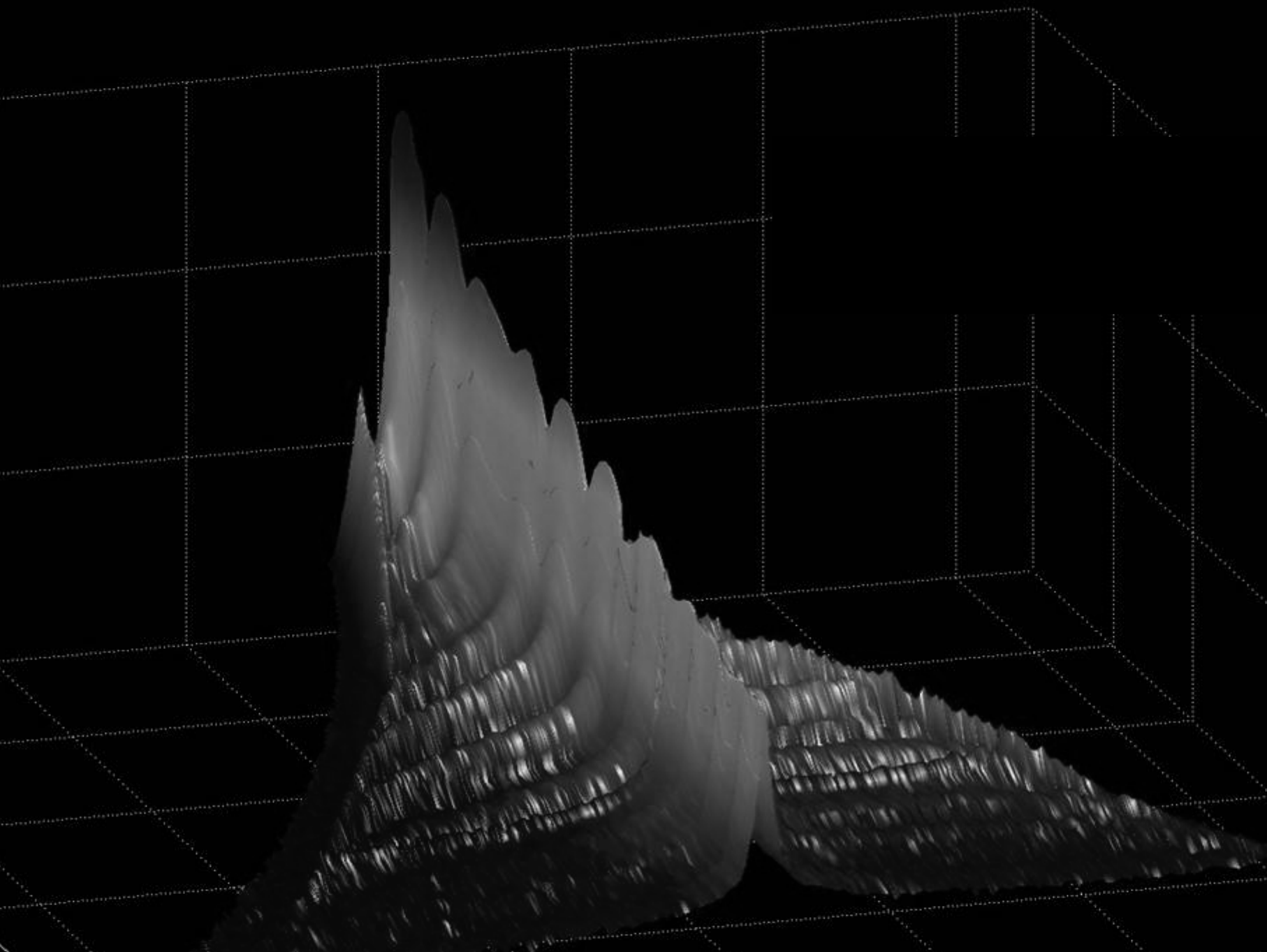
Asymmetric relaxation: Reciprocal space maps of test structures: $10\ \mu\text{m} \times 0.5\ \mu\text{m}$



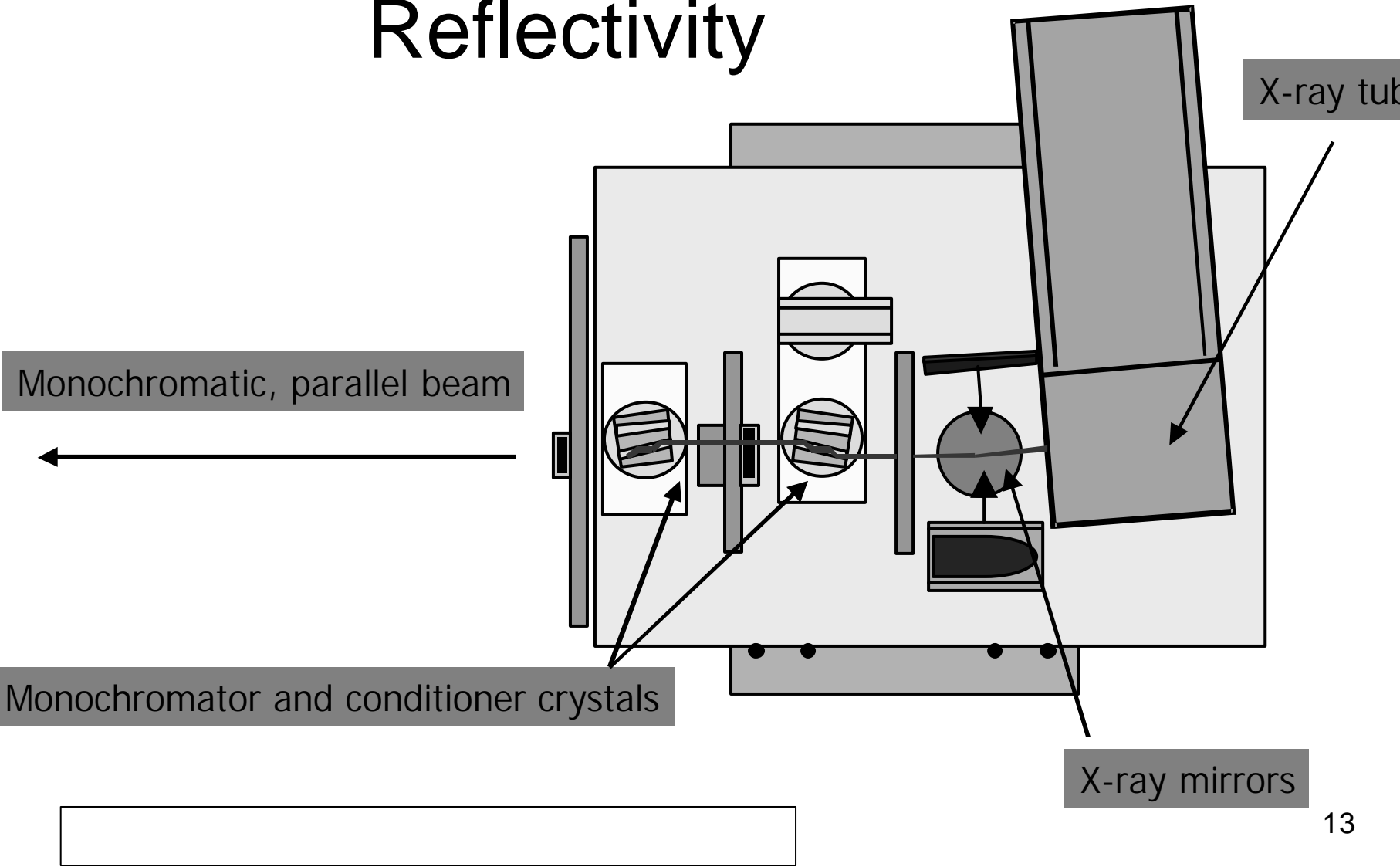
MgO Tunnel Junction for Spintronics Applications

Is there a change in the MgO interface structure when the bottom Co layer has a monolayer of CoO deposited?





X-ray Optics for Reflectivity



X-ray Optics for Reflectivity

- Remove crystal monochromator
- Use slit to define wavelength dispersion

Monochromatic, parallel beam

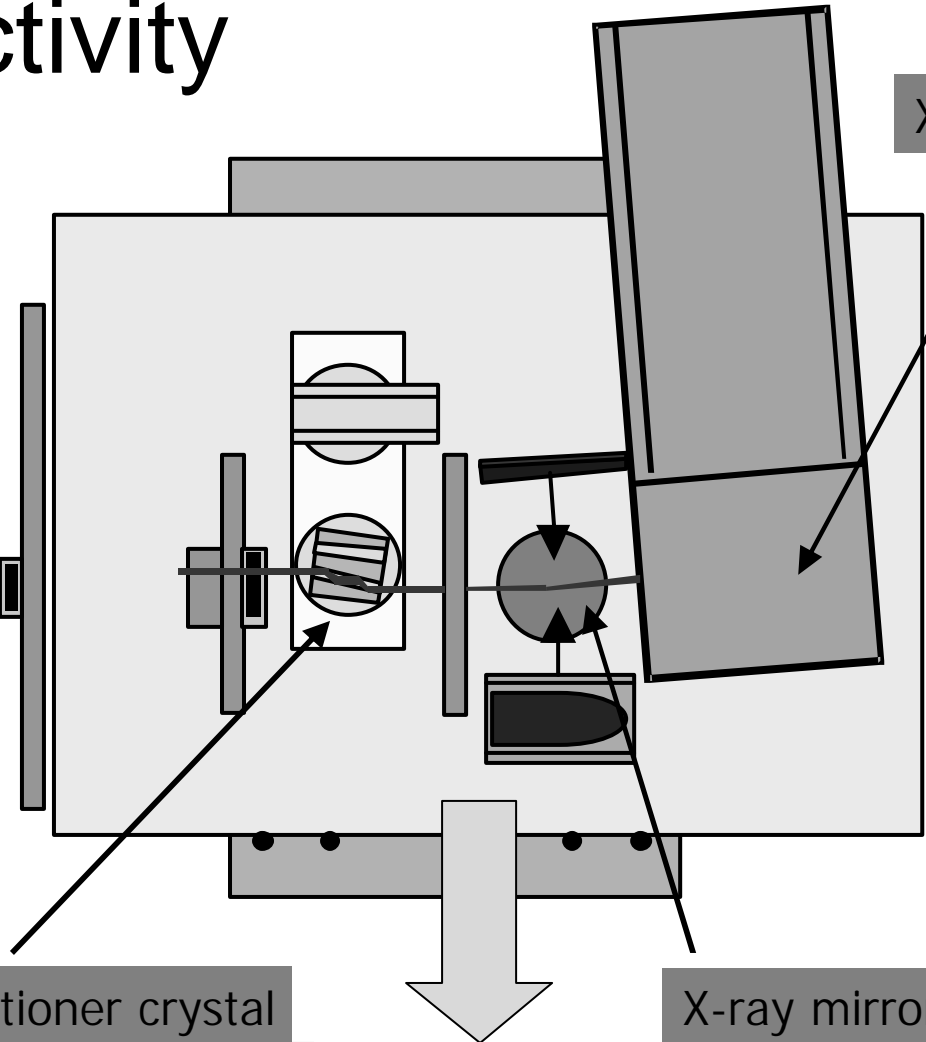


Slit monochromator

Conditioner crystal

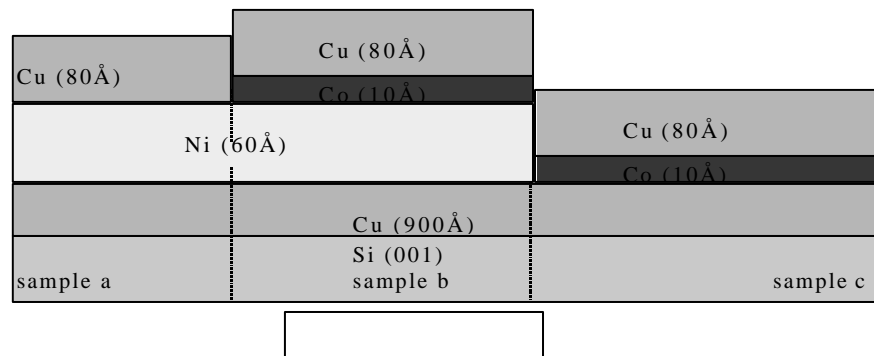
X-ray mirrors

X-ray tube



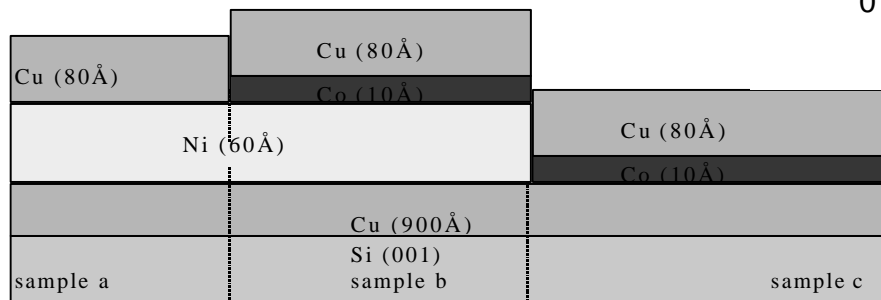
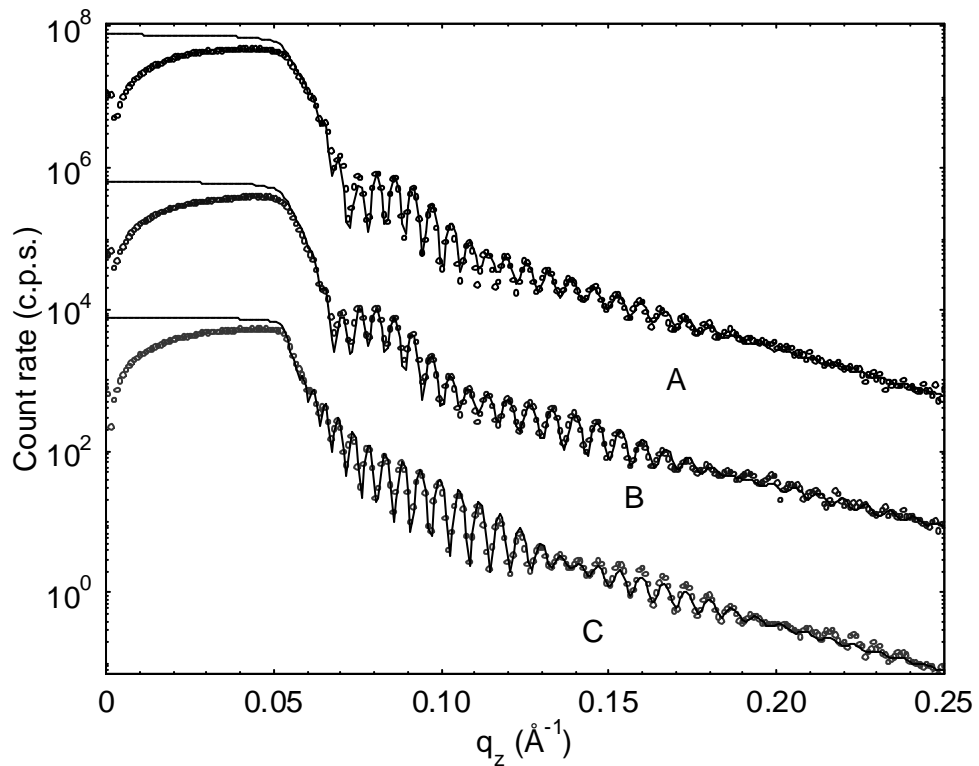
Ultra-thin transition metal films grown by Molecular Beam Epitaxy

- Shadow masks used to create three samples with identical Cu and (where appropriate, Ni and Co) thickness
- Polarized neutron reflectivity analysis of magnetic moments
- Need precise layer thickness to reduce number of free fitting parameters in PNR analysis



Ultra-thin Films - Specular Reflectivity

	Sample A	Sample B	Sample C
Cu cap thickness (Å)	75	82	84
Co thickness (Å)	-	11	10
Ni thickness (Å)	64	61	-
Cu thickness (Å)	830	823	840





Scientific Conclusions

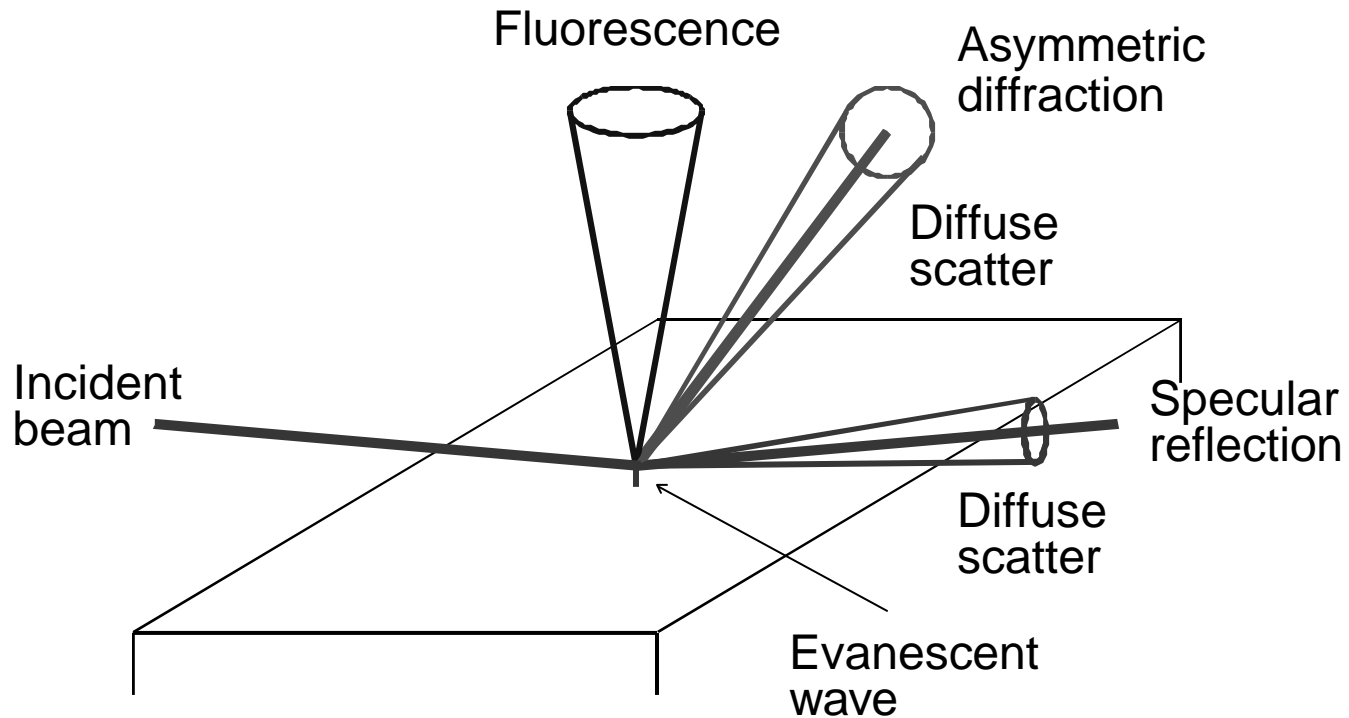
- Precise measurement of magnetic moment possible due to restricting parameter space
- Per Ni atom, $0.58 \pm 0.03 \mu_B$ and $0.59 \pm 0.03 \mu_B$ for Ni/Cu and Co/Ni/Cu samples
- No effect of interface environment detected

C.A.Vaz, G.Lauhoff, J.A.C. Bland, S.Langridge, D Bucknall, J Penfold, J.Clarke, S.K.Halder and B.K.Tanner, J. Magn. Mag. Mater. **313** (2007) 89-97

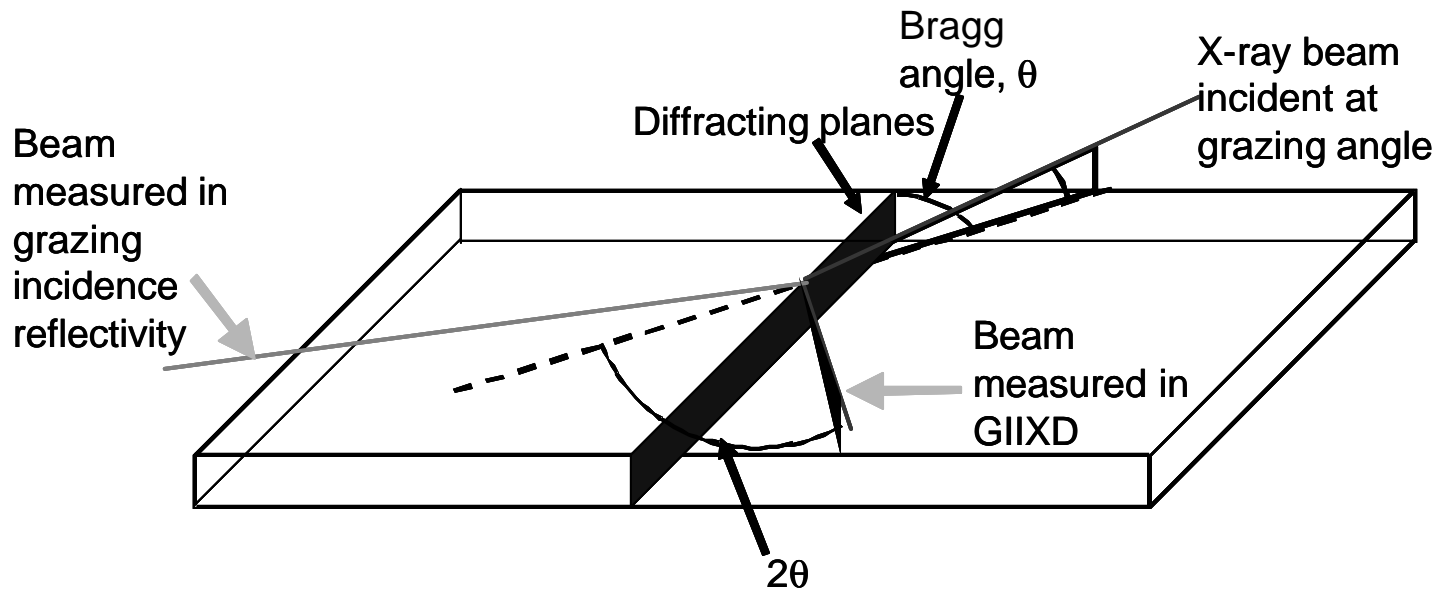
Another example of need to determine layer thickness

Measurement of hot electron momentum relaxation times in metals by femtosecond ellipsometry
V.V. Kruglyak, R.J. Hicken, M. Ali, B.J. Hickey, A.T.G.Pym and B.K.Tanner, Phys Rev B 71 (2005) 233104

Grazing incidence X-ray scattering

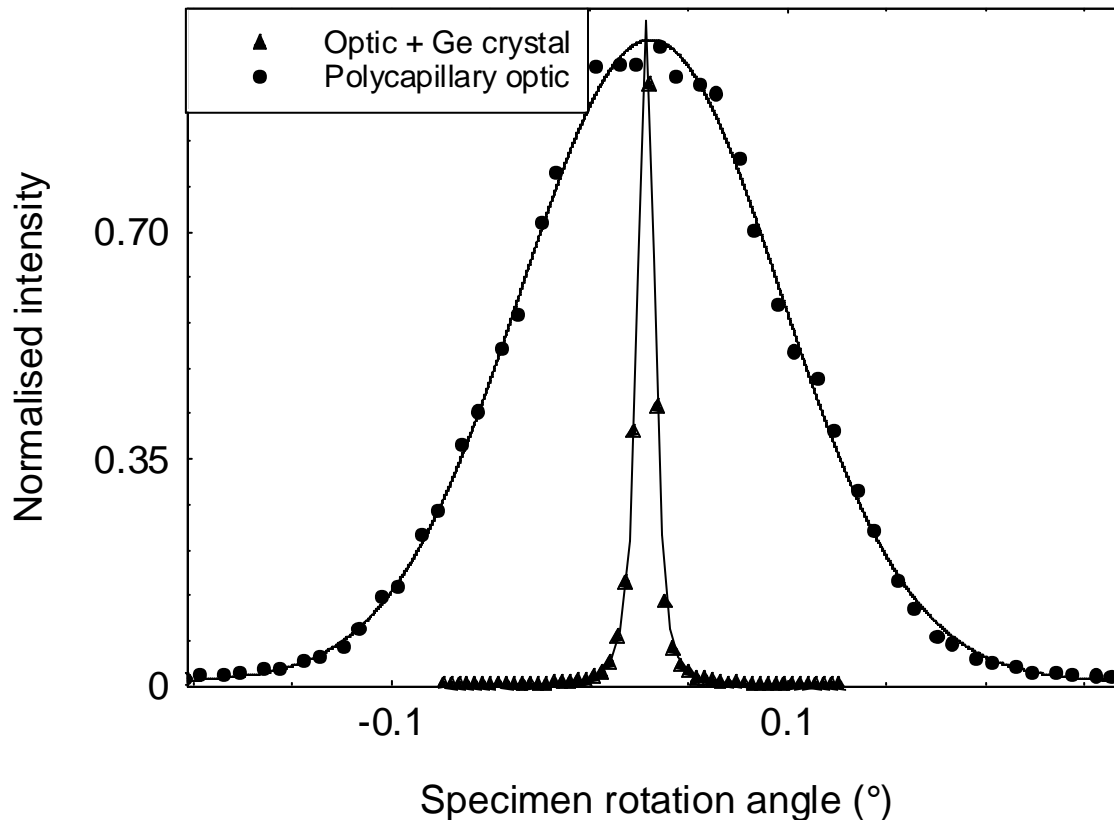


Principle of Grazing Incidence In-plane X-ray Diffraction



- Bragg planes normal to the sample surface
- Probes in-plane lattice parameter (in-plane strain)
- Probes in-plane mosaic
- Probes in-plane length scale

High Resolution GIIXD

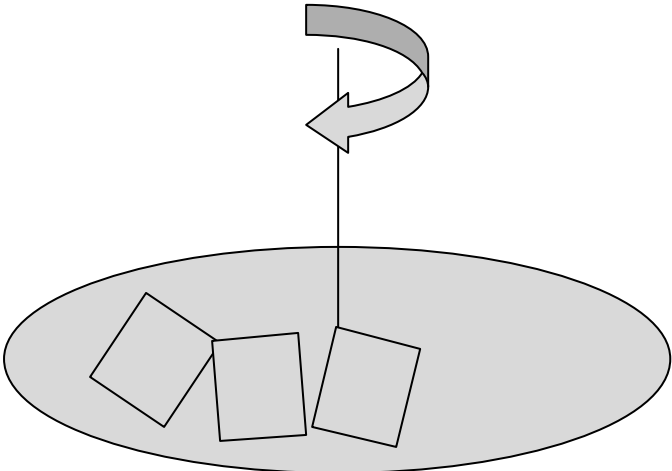
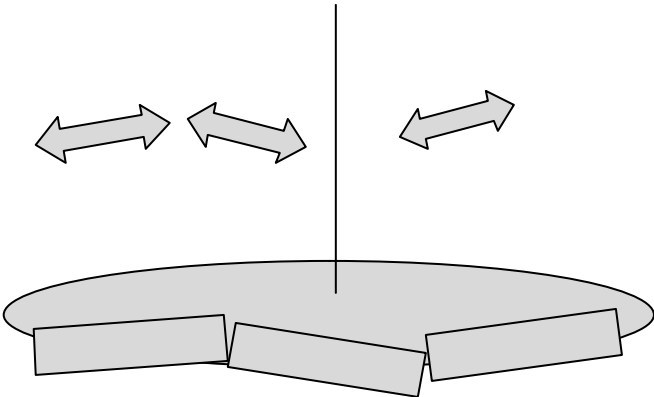


(Rocking curve) scans of the Si specimen about its surface normal, with the detector set for the 220 reflection, with and without the Ge monochromator crystal. Solid lines are fits of Voigt functions to the data.



Tilt and Twist Mosaic

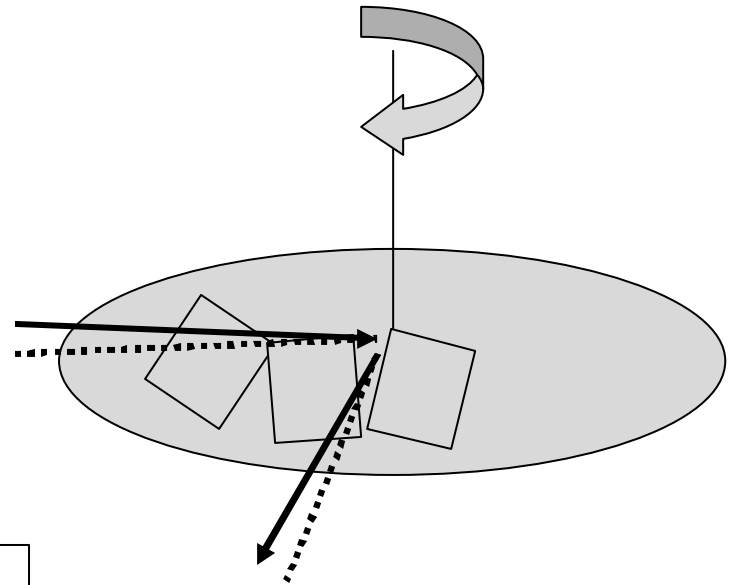
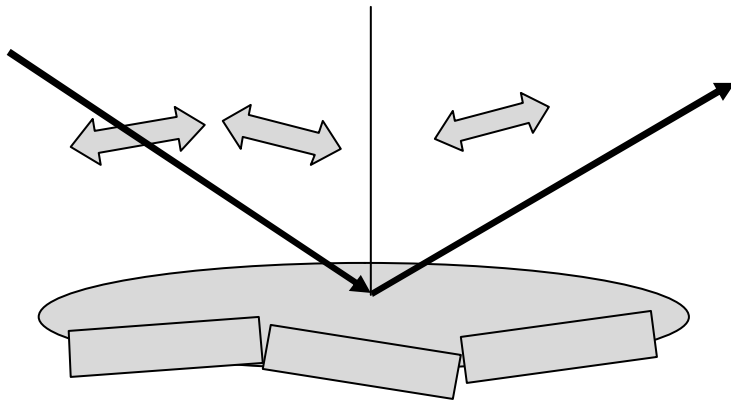
Tilt is misorientation **out of** the wafer plane
Twist is the misorientation **in** the wafer plane



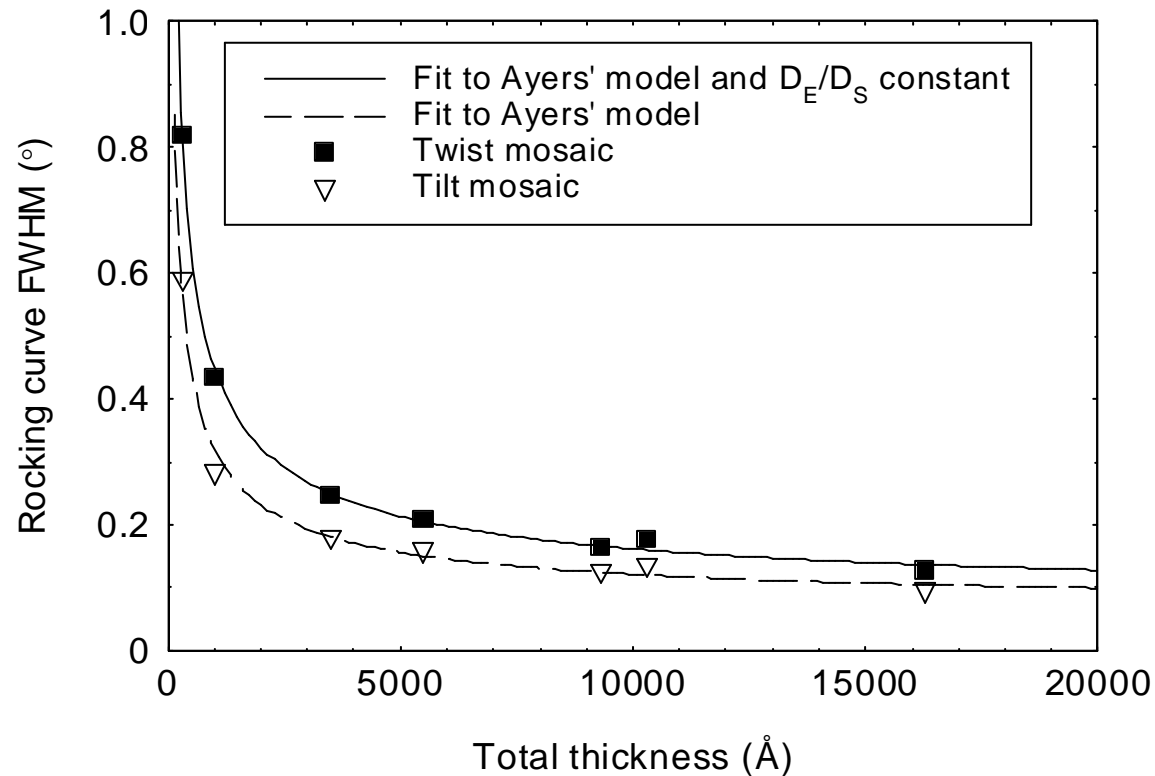
Tilt and Twist Mosaic

Tilt is misorientation **out of** the wafer plane

Twist is the misorientation **in** the wafer plane

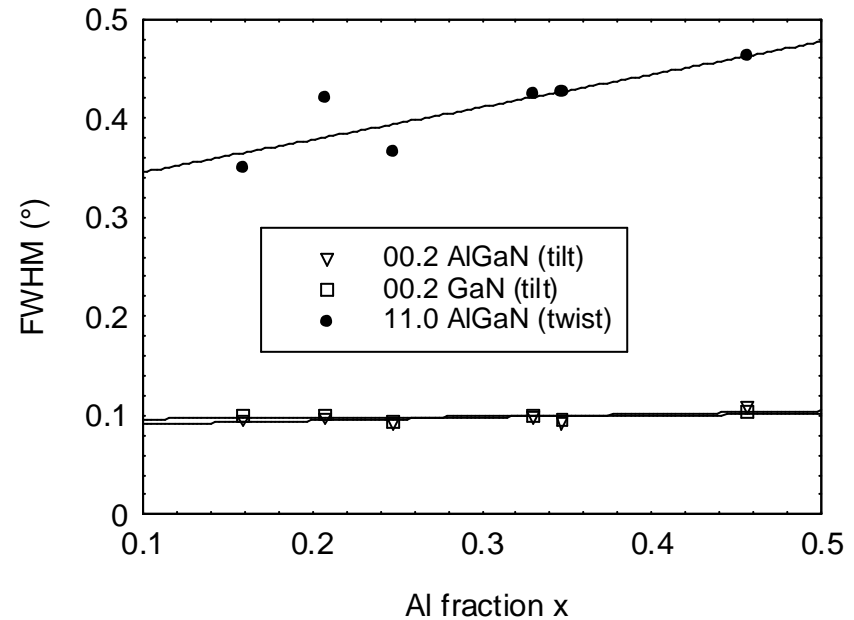
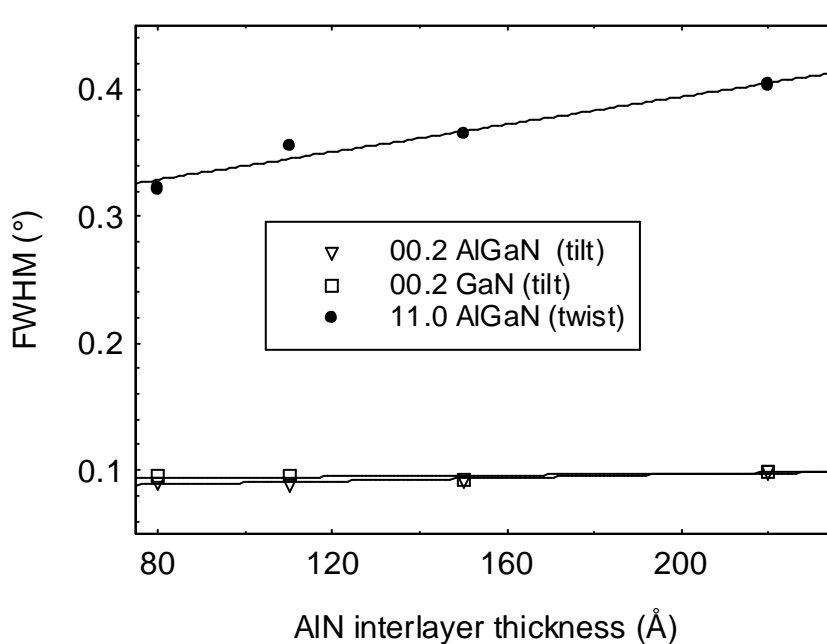


Twist and Tilt Mosaic as a Function of GaN Layer Thickness



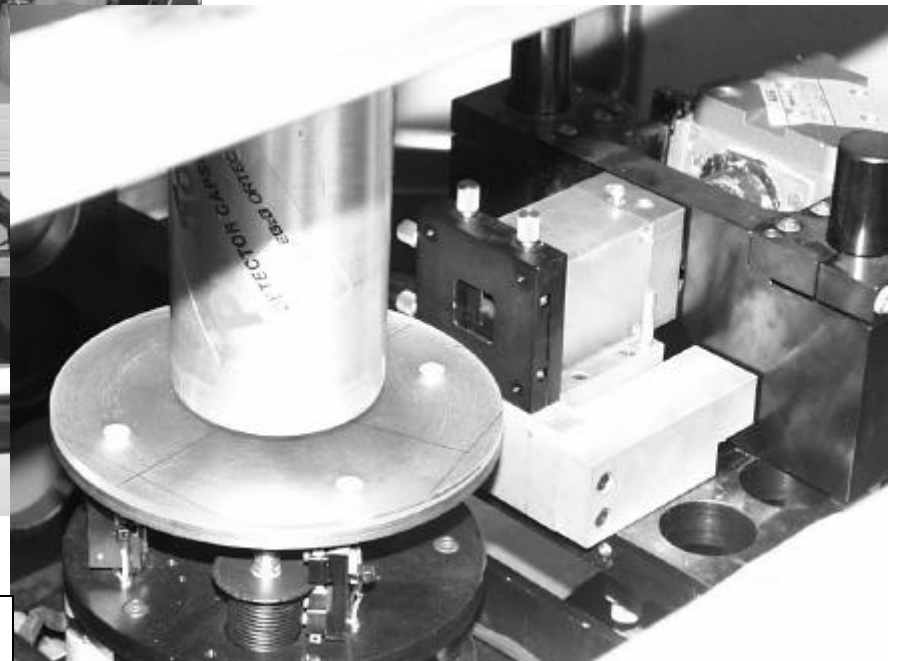
Ratio of number of threading screw to threading edge dislocations constant

Twist and Tilt Mosaic in Sapphire/GaN/AlN/ $\text{Al}_x\text{Ga}_{1-x}\text{N}$

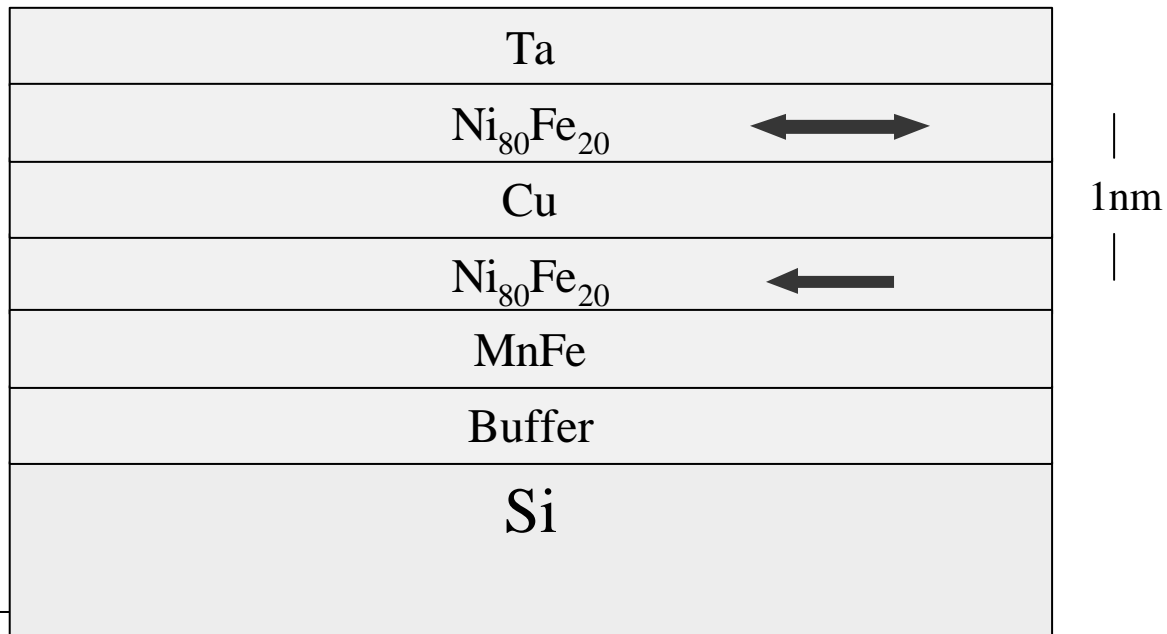


AlN interlayer between micron thick GaN and $\text{Al}_x\text{Ga}_{1-x}\text{N}$ layers. MOVPE. No change in the tilt mosaic (threading screw dislocation density) with thickness or Al fraction x of the upper layer. A linear increase in the twist mosaic (threading edge dislocation density) was observed as a function of interlayer thickness and x. For all samples the twist mosaic of the AlGaN was significantly greater, by at least a factor of two, than that of the GaN layer.

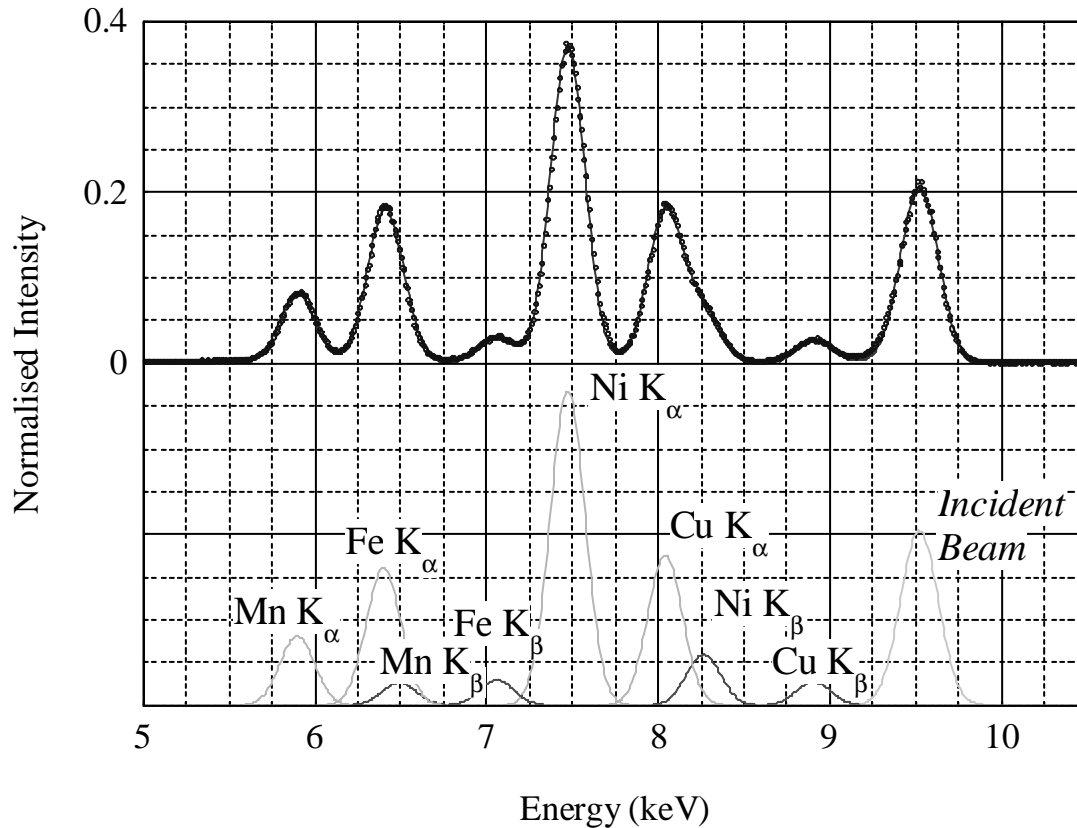
Durham reflectometer with fluorescence attachment



Spin Valve Structure for Spintronics Applications



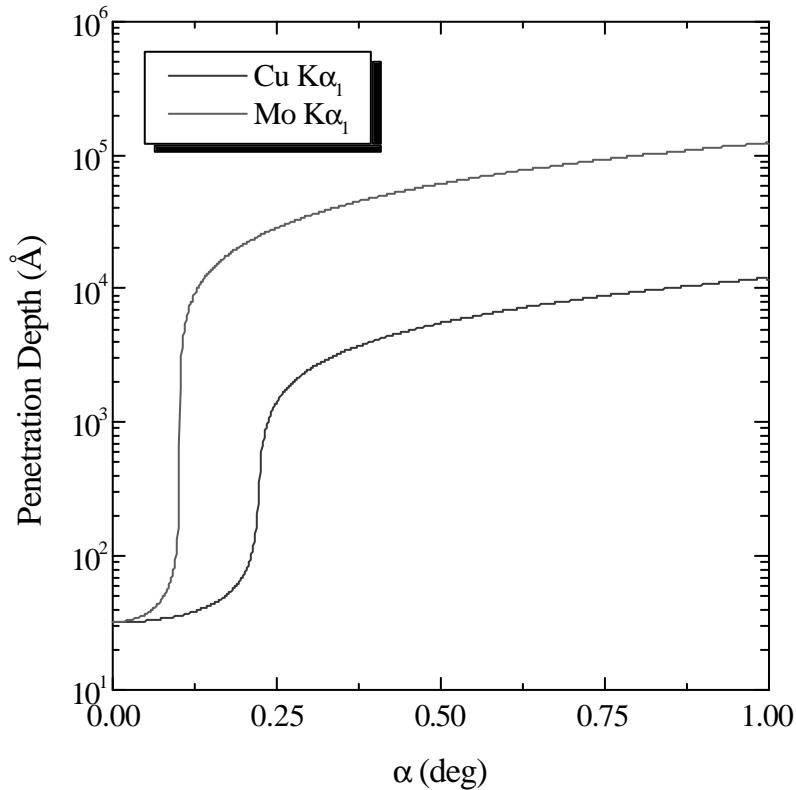
Grazing Incidence Fluorescence from Spin Valve Structures



- Deconvolution from Gaussian peaks
- Measure area under peaks



Grazing Incidence Fluorescence Analysis of Bi as a Surfactant



Penetration depth L is

$$L = \lambda / \{ \pi(\alpha_c^2 - \alpha^2) \}^{1/2}$$

where α_c is the critical angle for total external reflection

As the incidence angle rises, penetration of wave increases.

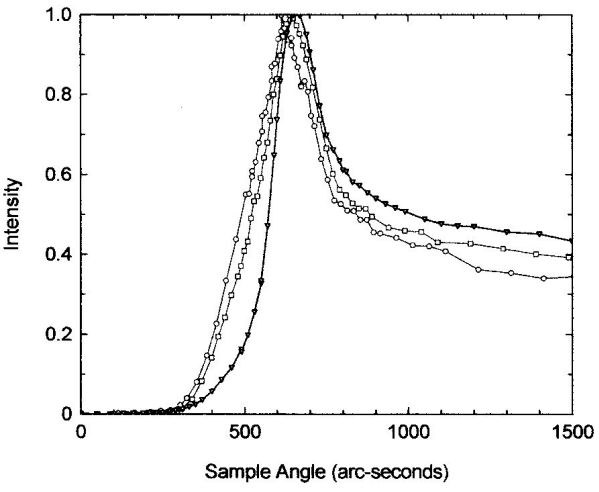
Around critical angle, very high sensitivity to depth

- **Evanescent wave below critical angle**
- **Used MoK radiation to excite Bi**



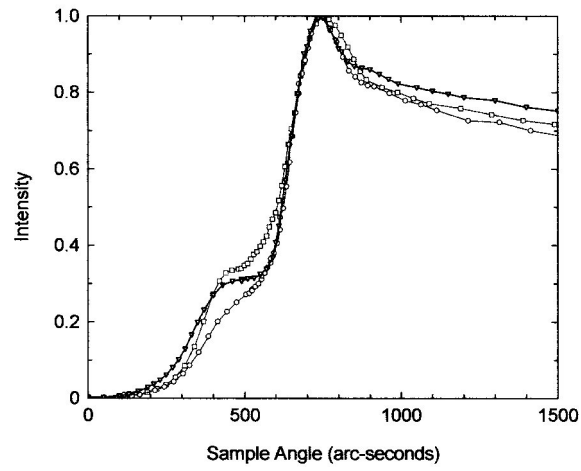
Normalized Grazing Incidence Fluorescence Data

Bi Fluorescence

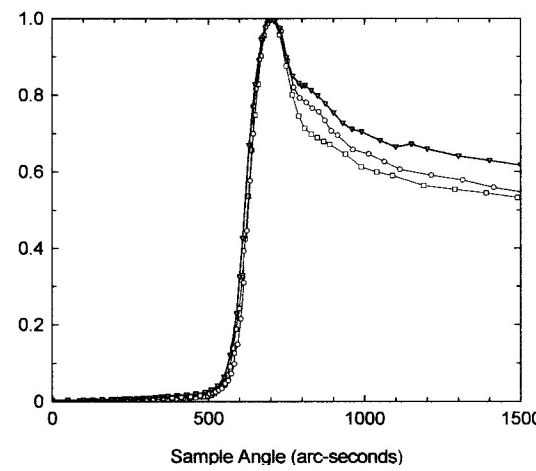


— A7 Experimental Data
— A5 Experimental Data
— A13 Experimental Data

Cu Fluorescence



Ni Fluorescence



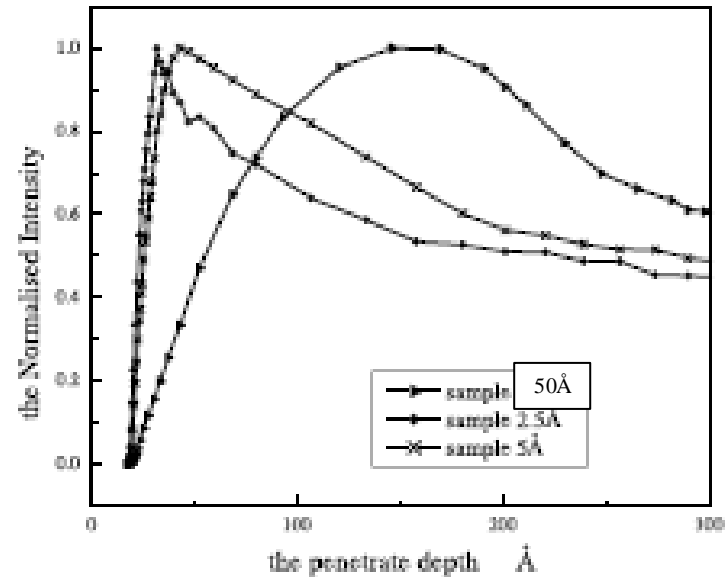
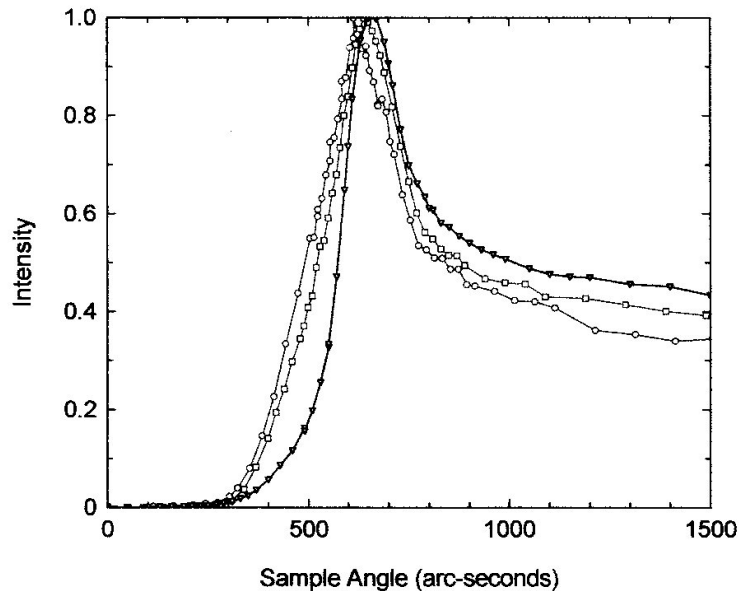
- Ni fluorescence almost independent of Bi thickness
- Cu fluorescence shows step at critical angle from



Normalized Grazing Incidence Bi Fluorescence Data

Bi moves to the surface for monolayer coverage
Bi stays low for thick layer

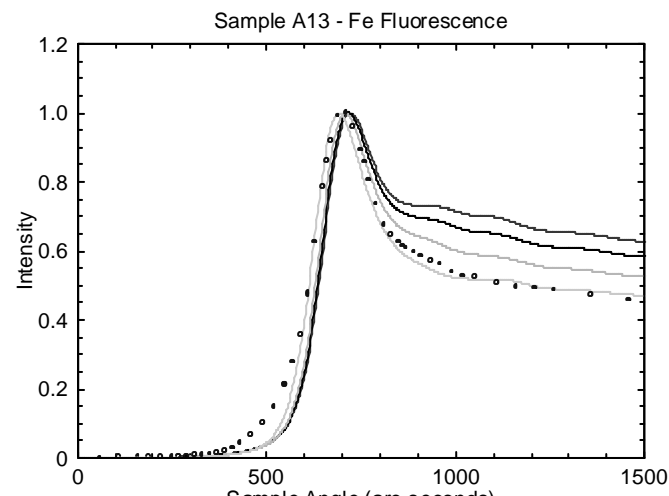
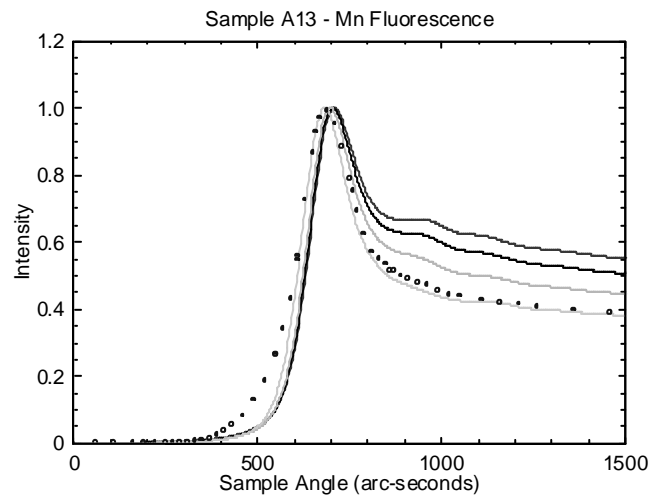
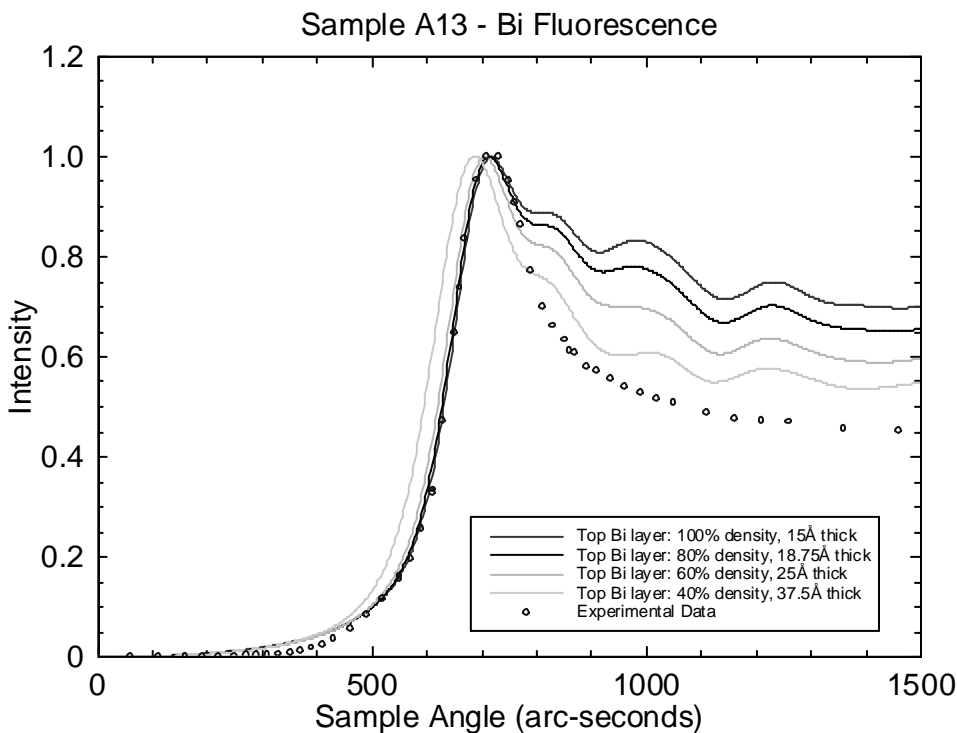
Bi Fluorescence



➤ Low Bi thickness – fluorescence rises at lower angle compared to thick layer

Grazing Incidence Fluorescence

Bi above and below FeMn

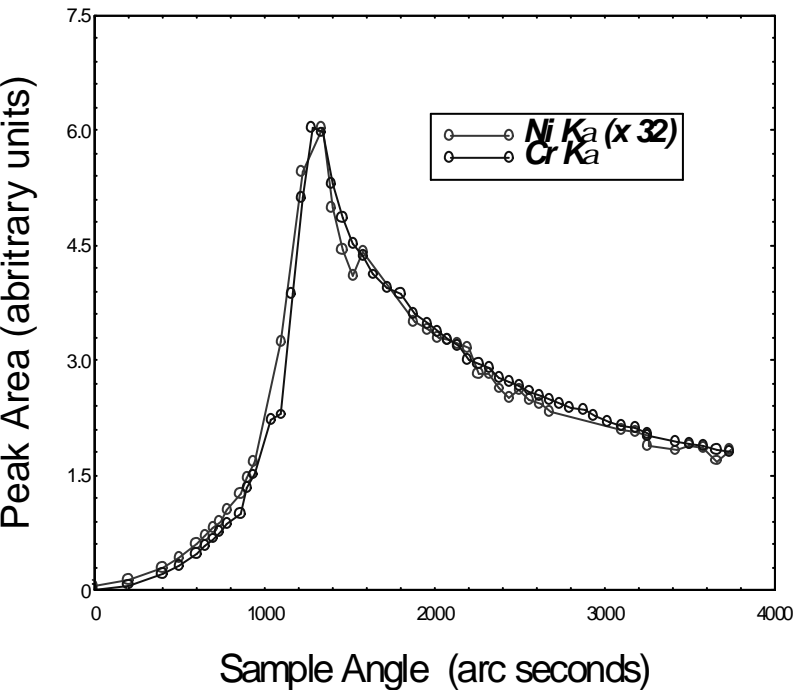


- **25Å Bi below FeMn, 25Å low density Bi above**
- **Detailed fitting difficult**

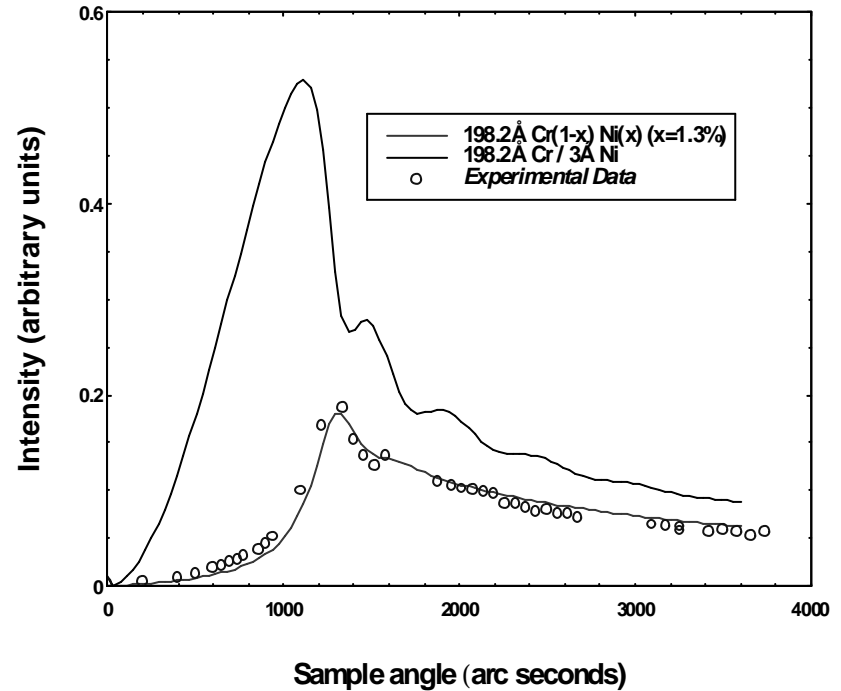
Fits to simulation of fluorescence yield as function of angle



Peak Areas from 200Å Cr Single Film



Simulations of Ni Fluorescence for Different Ni Contamination



Collaborators and Contributors

Bede plc

Paul Ryan

Tamzin Lafford

Matthew Wormington

Stéphane Godny

Keith Bowen

Durham University

Tom Hase

Alex Pym

David Eastwood

Stuart Wilkins (now at BNL)

Peter Parbrook (Univ of Sheffield)

Mai Zhenhong (CAS, Beijing)

Mark Goorsky (UCLA)

Bill Egelhoff (NIST)

Carlos Vaz (Univ of Cambridge)

Tony Bland (Univ of Cambridge)